ELSEVIER

International Journal of Mass Spectrometry 201 (2000) 1–15

International Journal of Mass Spectrometry

Systematic comparison of the benzynes, pyridynes, and pyridynium cations and characterization of the Bergman cyclization of *Z*-but-1-en-3-yn-1-yl isonitrile to the *meta* diradical 2,4-pyridyne

Stefan L. Debbert, Christopher J. Cramer*

Department of Chemistry and Supercomputer Institute, University of Minnesota, Minneapolis, MN 55455-0431, USA

Received 14 July 1999; accepted 21 September 1999

Abstract

The geometries and relative energies of the singlet and triplet states of the three didehydrobenzenes (benzynes), six didehydropyridines (pyridynes), and six didehydropyridinium (pyridynium) cations are compared at the density functional, multiconfigurational self-consistent field, and coupled cluster levels of theory. The title Bergman cyclization, which produces a *meta* diradical, is characterized at the density functional theory level and compared to the analogous Bergman cyclizations generating all of the *para* diradicals in the subject aryne series. Singlet–triplet splittings in the pyridynium cations and ^{1}H hyperfine couplings in the *N*-protonated pyridyl radicals are found to be well correlated by proportionality constants determined previously for other arynes. Heats of formation (298 K) are predicted for all six pyridynes. (Int J Mass Spectrom 201 (2000) 1–15) © 2000 Elsevier Science B.V.

Keywords: Aryne; Didehydroarene; Biradical; Enediyne cyclization; Singlet-triplet splitting

1. Introduction

Enediyne and related antitumor antibiotics effect the double-stranded cleavage of DNA. Since the discoveries that the reactive intermediates formed from these drugs include *p*-benzyne- [1,2], didehydroindene- [3,4], and α,3-dehydrotoluene-type [5,6] biradicals, considerable effort has been expended to further understand the electronic structure, and potentially thereby optimize the *in vivo* activity [7], of didehydroarenes (arynes). A key goal in this regard is controlling the reactivity/selectivity of the hydrogen-atom-abstraction processes whereby these biradical intermediates function [8]. Chen and co-workers have advanced a simple model addressing this issue. They correlate the reactivity of singlet-state biradicals with the magnitude of their singlet–triplet (ST) energy splittings, ΔE_{ST}; the larger the splitting, the greater the barrier for H-atom abstraction and, hence, the more selective the biradical [9–11]. In principle, then, understanding what controls the magnitude of ST splittings in biradicals can facilitate the rational design of more selective DNA-cleaving agents.

Systematic theoretical studies of all possible arynes derived from a single aromatic parent molecule have appeared for the three didehydrobenzenes [12–

---

* Corresponding author. E-mail: cramer@pollux.chem.umn.edu

PII S1387-3806(00)00160-3

18] (benzynes) and ten didehydronaphthalenes [17,19] (naphthalynes). The effect of heteroatom incorporation into the aromatic ring has been examined for the six didehydropyridines [20,21] (pyridynes). Substantial experimental data on the structure and reactivity of various members of the benzyne, naphthalyne, and pyridyne families have also been reported [11,22–52].

Much less well characterized has been the influence of charge on aryne properties. Thoen and Kenttämaa [49,52] have provided gas-phase data for *N*-arylated pyridinium ions where the arylating substituent is a benzyne, and Hoffner et al. [11] and Cramer [53] have characterized certain aspects of the structure and reactivity of *N*-protonated 2,5-didehydropyridine. One purpose of this article is to extend that record by systematically characterizing the six *N*-protonated didehydropyridinium cations (pyridyniums) at levels of electronic structure theory previously employed for the isoelectronic benzynes and pyridynes in order to better understand the influence of charge and heteroatom effects on biradical structures and energetics.

Aromatic biradicals pose a number of interesting challenges to computational technology [11,13–17, 19–21,53–63]. Single-determinant levels of theory (e.g. Hartree-Fock) are generally inappropriate for systems whose two frontier orbitals are nearly degenerate, as is the case with arynes characterized by small ST splittings, since important nondynamical correlation effects are neglected. These effects can be accounted for by multireference self-consistent-field (MCSCF) calculations, but in order to calculate state energy splittings to chemically useful levels of accuracy, dynamical correlation effects must also be taken into account.

In this article, we apply several levels of theory, including multireference second-order perturbation theory (CASPT2), density functional theory (DFT), and coupled-cluster theory including all single, double, and perturbatively estimated triple excitations using single-determinant reference wave functions expanded in both Hartree-Fock [CCSD(T)] and Brueckner [BCCD(T)] orbitals. One of the pyridynium singlets required the use of Brueckner orbitals to overcome an instability in estimating the effects of triple excitations otherwise inherent in the CCSD(T) approach.

We compare the structures and relative energies of the benzynes, pyridynes, and pyridyniums at consistent levels of theory. We discuss inter alia the role of the nitrogen lone pair, protonated or not, in the thermodynamics of these isomers, and the sensitivity of the singlet–triplet gap to the distance between the radical centers. We also provide a DFT characterization of the Bergman cyclization [64] pathway by which *Z*-but-1-en-3-yn-1-yl isonitrile generates 2,4-pyridyne; this is a unique reaction in the sense that Bergman cyclizations typically generate *para*-related diradicals, not *meta*-related ones. Finally, we examine ^{1}H isotropic hyperfine splittings in the *N*-protonated pyridyl radical cations to determine if they correlate with singlet–triplet splittings in corresponding pyridynium cations as previously observed for analogous radicals/arynes in the benzyne [17,19], naphthalyne [17,19], pyridyne [21], and didehydroquinone [63] series.

2. Computational methods

Molecular geometries for all arynes were optimized at the MCSCF and DFT levels of theory using the correlation-consistent polarized valence-double-ζ (cc-pVDZ) basis set [65]. The geometries of *Z*-but-1-en-3-yn-1-yl isonitrile and its Bergman cyclization transition state structure were optimized only at the DFT level.

The MCSCF calculations were of the complete active space (CAS) variety [66]. CAS geometry optimizations were carried out for the benzynes and pyridynium cations employing an eight-electron/eight-orbital active space comprised of the six π orbitals and the two nonbonding σ orbitals. Active spaces reduced by one and two electrons/orbitals were used for optimization of the benzyl and *N*-protonated pyridyl radicals, and benzene and *N*-protonated pyridinium cation, respectively. Analogous active spaces in the pyridyne series also included the nitrogen lone pair (additional two electrons/one orbital).

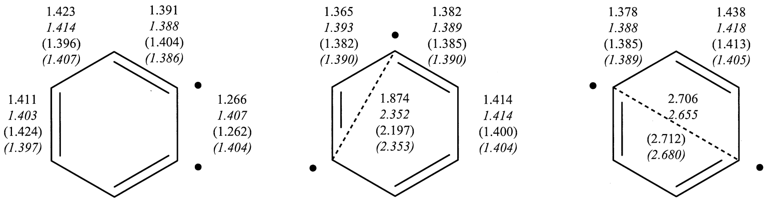

Fig. 1. Calculated heavy-atom bond lengths and biradical separations (angstroms) for singlet and triplet (in parentheses) benzyne isomers at the BPW91/cc-pVDZ and CAS(8,8)/cc-pVDZ (italics) levels of theory. The singlet *p*-benzyne DFT structure is from a broken-spin-symmetry calculation.

The DFT calculations employed the gradient-corrected functionals of Becke [67] and Perdew et al. [68] (BPW91). Both restricted and broken-spin-symmetry unrestricted DFT optimizations were carried out for those molecules exhibiting restricted singlet instability—this has been shown to give more accurate geometries for a number of relevant aromatic singlet biradicals [53,57,62,69]. The natures of all DFT stationary points were confirmed by computation of analytic vibrational frequencies, which were also used to compute zero-point vibrational energies (ZPVE) and 298 K thermal contributions to enthalpies. Total spin expectation values for Slater determinants formed from the optimized (unrestricted) Kohn-Sham orbitals did not exceed 0.76 and 2.02 for the monoradicals and biradical triplets, respectively.

Dynamic electron correlation using the CAS reference was accounted for at the CASPT2 level [70–72]. Some caution must be applied in interpreting the CASPT2 results since this level of theory is known to suffer from a systematic error proportional to the number of unpaired electrons [71]. Coupled-cluster calculations for single-configuration reference wave functions expanded in Hartree-Fock {CCSD(T) [73,74]} or Brueckner {BD(T) [75]} orbitals were also carried out including all single and double excitations and a perturbative estimate for triple excitations. Brueckner orbitals eliminate contributions from single excitations in the coupled cluster ansatz, and this alleviates instabilities [76] associated with very large singles amplitudes in the more common CCSD(T) method that have previously been observed in aromatic biradicals having low degrees of symmetry [53]. BCCD(T)/cc-pVDZ and CCSD(T)/cc-pVDZ calculations were of the single-point variety.

Isotropic hyperfine coupling constants (hfs) were calculated as [77]

$$a_X = (4\pi/3)\langle S_z\rangle^{-1} g g_X \beta \beta_X \rho(X) \tag{1}$$

where g is the electronic g factor, β is the Bohr magneton, g_X and β_X are the corresponding values for nucleus X, and $\rho(X)$ is the Fermi contact integral

$$\rho(X) = \sum_{\mu\nu} P_{\mu\nu}^{\alpha-\beta} \phi_\mu(\mathbf{R}_X) \phi_\nu(\mathbf{R}_X), \tag{2}$$

where $\mathbf{P}^{\alpha-\beta}$ is the BPW91/cc-pVDZ one-electron spin density matrix, and evaluation of the overlap between basis functions ϕ_μ and ϕ_ν is only at the nuclear position, $\mathbf{R}_X$.

All multireference and single-reference calculations were carried out with the MOLCAS [72] and GAUSSIAN 94 [78] electronic structure program suites, respectively.

3. Results and discussion

The DFT and CAS(8,8) optimized heavy-atom bond lengths for the singlet and triplet states of the benzynes, pyridynes, and pyridynium cations are provided in Figs. 1–3. The energies of all of the biradicals relative to their singlet 3,4-isomers (the lowest energy isomer in each case) are collected in Table 1 for the different levels of theory. We first discuss the pyridynium cations, as these have not seen prior computational study as a complete isomeric series. We then compare the benzynes, pyridynes, and

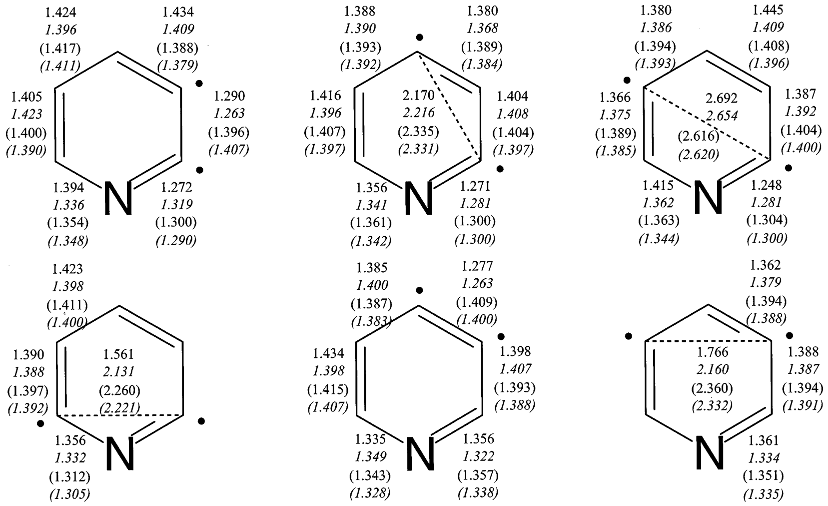

Fig. 2. Calculated heavy-atom bond lengths and biradical separations (angstroms) for singlet and triplet (in parentheses) pyridyne isomers at the BPW91/cc-pVDZ and CAS(8,8)/cc-pVDZ (italics) levels of theory.

pyridyniums to one another at consistent levels of theory so as to elucidate the effects of heteroatom and/or charge incorporation on structures and energetics.

3.1. Pyridynium cations

We note that, at least for molecular geometries, DFT appears to successfully account for dynamical electron correlation (by construction of the functional) lacking at the CAS(8,8) level. We come to this conclusion since absolute energies calculated at the CASPT2 level are lower for the DFT geometries than for the CAS(8,8) geometries for all structures other than singlet 3,5-pyridynium (data not shown)—the 3,5-singlet is one of two special cases discussed further below. Unless otherwise specified, we there-

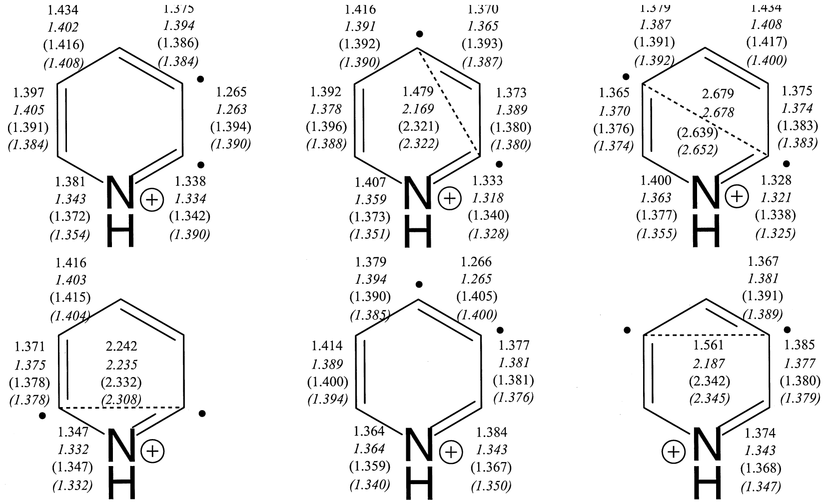

Fig. 3. Calculated heavy-atom bond lengths and biradical separations (angstroms) for singlet and triplet (in parentheses) pyridynium cation isomers at the BPW91/cc-pVDZ and CAS(8,8)/cc-pVDZ (italics) levels of theory. The 2,6- and 3,5-singlet DFT structures are from broken-spin-symmetry calculations.

Table 1
Relative energies (kcal/mol) of arynes relative to their respective singlet global minima at various levels of theory

	Singlets						Triplets					
Theory[a]	2,3	2,4	2,5	2,6	3,4[b]	3,5	2,3	2,4	2,5	2,6	3,4	3,5
Benzynes[c]	*ortho*	*meta*	*para*	*meta*	*ortho*	*meta*	*ortho*	*meta*	*para*	*meta*	*ortho*	*meta*
BPW91			29.8	8.7	0.0				26.7	27.9	31.8	
CASPT2			21.7	10.1	0.0				26.3	27.6	30.8	
CCSD(T)			27.2	14.6	0.0				28.8	32.4	33.1	
Pyridynium cations												
BPW91	8.9	3.9	25.4	23.2	0.0	6.1	33.5	28.7	29.3	31.1	32.1	29.8
CASPT2	8.6	10.1	24.5	20.3	0.0	12.8	32.7	28.4	29.2	30.7	31.5	29.9
CCSD(T)	9.4	10.6	26.0[d]	22.8	0.0	14.4	35.1	32.2	31.8	34.6	33.5	33.7
Pyridynes[e]												
BPW91	5.1	3.9	13.1	21.5	0.0	15.2	23.0	27.2	26.8	18.1	35.9	27.4
CASPT2	7.1	1.2	11.3	17.5	0.0	14.7	21.7	24.5	24.0	14.9	33.5	28.2
CCSD(T)	5.9	4.9	14.5	21.1[f]	0.0	18.7	24.8[g]	28.7	26.3	20.6	34.2	31.8

[a] CASPT2 results are for CAS(8,8) geometries; CCSD(T) results are for BPW91 geometries unless otherwise noted. See Figs. 1–3 for geometries.

[b] Absolute energies (h) for this column: −230.902 76, −230.195 45, −230.262 47; −247.297 32, −246.518 17, −246.629 32; −246.950 03, −246.166 11, −246.277 20.

[c] For convenience, the relationship between the three benzyne isomers and the six pyridyne(ium) isomers is indicated.

[d] BCCD(T) relative energy.

[e] See [21]; note that for consistency the CCSD(T) numbers do *not* include contributions from CCSD/cc-pVTZ calculations and thus differ from those in [21].

[f] CAS(8,8) geometry.

[g] This value appears in [21], where it is incorrect. The corresponding value in [21] should be 26.8 kcal/mol.

fore report all coupled-cluster energetic data *only* for the DFT geometries. We note that the broken-spin-symmetry geometries of the 2,5- and 2,6-pyridynium cations (the only isomers with restricted singlet instabilities) were predicted to be from 1 to 4 kcal/mol lower than their respective restricted geometries at various levels of theory; no single geometrical coordinate shows a particularly large change in either instance. As a final technical point, we found that, in most cases, the differences between the absolute energies computed at the BCCD(T) and CCSD(T) levels were small. For all singlets with the exception of the 2,5-singlet, the average difference was 0.4 kcal/mol, with the CCSD(T) energy being the lowest in every case. For all triplets, the average difference was 0.8 kcal/mol, with the BCCD(T) energy being the lowest in every case. The systematic nature of the differences implies that ST splittings predicted at the BCCD(T) level must on average be 1.2 kcal/mol larger than those predicted at the CCSD(T) level. Given the present paucity of experimental data, however, there is not yet any way to judge which is the most accurate. The failure of CCSD(T) theory for the 2,5-singlet has been discussed elsewhere [53], so no comparison to that level is possible for this isomer.

Fig. 3 illustrates two particularly large differences in geometric predictions between the DFT and CAS(8,8) levels of theory. In particular, DFT predicts the 2,4- and 3,5-singlets to have bicyclic structures with bond lengths between the dehydrocarbons of 1.479 and 1.561 Å, respectively. At the CAS(8,8) level, on the other hand, “typical” aromatic six-membered ring structures are maintained, with non-bonded separation of the two dehydrocarbons exceeding 2.1 Å. In this instance, the ring contraction appears to be a function of dynamical electron correlation that is included in the DFT Hamiltonian but absent in the MCSCF process—the bicyclic 2,4- and 3,5-singlet DFT structures are predicted to be lower in energy than their CAS(8,8) counterparts by 2.4 and

Table 2
ST splittings (H_0, kcal/mol) of arynes at various levels of theory

	Benzynes[a]			Pyridynium cations						Pyridynes[b]					
Theory[c]	*ortho*	*meta*	*para*	2,3	2,4	2,5	2,6	3,4	3,5	2,3	2,4	2,5	2,6	3,4	3,5
BPW91	−31.3	−19.4	2.0	−24.1	−24.8	−4.3	−8.1	−31.5	−24.0	−17.9	−23.4	−14.0	2.1	−35.2	−12.9
CASPT2	−30.4	−18.0	−5.8	−23.6	−18.3	−5.2	−10.6	−30.9	−17.5	−14.6	−23.3	−13.0	1.2	−32.9	−14.2
CCSD(T)	−32.6	−18.3	−2.8	−25.2	−21.5	−5.6[d]	−12.1	−32.9	−19.6	−18.9	−25.1	−12.9	−0.3[e]	−34.4	−14.8
Expt.[f]	−37.5	−21.0	−3.8												
	±0.3	±0.3	±0.5												

[a] BPW91 and CASPT2 data from [17].

[b] See [21]; note that for consistency the CCSD(T) numbers do *not* include contributions from CCSD/cc-pVTZ calculations and thus differ from those in [21].

[c] CASPT2 results are for CAS(8,8) geometries; CCSD(T) results are for BPW91 geometries unless otherwise noted; ZPVE from BPW91 level. See Figs. 1–3 for geometries.

[d] BCCD(T) splitting.

[e] CAS(8,8) geometry for singlet.

[f] [51].

1.8 kcal/mol at the CCSD(T) level. Of course, one might worry that these energy differences at the CCSD(T) level reflect primarily cumulative contributions from coordinates *other* than the distance between the two dehydro centers. To test this point, and moreover to establish whether the didehydro separation has a single-well potential or a double-well potential, constrained optimizations of structures along a putative didehydro bond stretching coordinate were carried out for the 2,4-singlet at a variety of theoretical levels. Interestingly, at the CAS(8,8) level a stationary bicyclic structure for the 2,4-singlet *can* be found, with a bond length between the two dehydrocarbons of 1.490 Å, but it is higher in energy than the monocyclic structure by 8.3 kcal/mol. No other level of theory provides support for there being two stationary structures, however, and the CCSD(T)//BPW91 and CASPT2//BPW91 coordinates both show minima much closer to the DFT bicycle than to the CAS(8,8) monocycle.

The issue of bicyclic structures is a particularly thorny one that has been addressed for many *meta*-arynes [16,20,21,51,55,57]. Apparently erroneous bicyclic structures have most often been observed at the Hartree-Fock level, where they arise from an artifact associated with this level being a single-determinantal level of theory. When nondynamical correlation is included at the MCSCF level, the bicyclic structures inevitably open to monocyclic ones. However, this tendency appears to be opposed by energetic effects associated with dynamical correlation, so that individual *meta*-arynes can be highly fluxional. A most remarkable example is found in Fig. 2, where the DFT and CAS structures for 3,5-pyridyne are predicted to differ by only 0.03 kcal/mol at the CCSD(T) level in spite of having dehydrocarbon separations that differ by almost 0.4 Å [21].

Turning now to energetic issues, we note first that for four of the six pyridynium isomers, the relative singlet and triplet energies are fairly insensitive to level of theory (Table 1). The exceptions are the 2,4- and 3,5-singlets, where the stability of the bicyclic structures appears to be overestimated by DFT, as judged by their considerably higher relative energies at the CCSD(T) level [note that it is purely coincidental that the relative energies of the bicyclic DFT structures at the CCSD(T) level are close to the relative energies of the monocyclic CAS structures at the CASPT2 level]. This phenomenon also occurs for *m*-benzyne, and is presumably related to artifacts associated with the single-determinantal nature of DFT (vide supra). Analysis of pyridynium relative energies, together with the data compiled in Tables 2 and 3, is most informative when evaluated in the context of the benzynes and pyridynes.

Table 3
Biradical stabilization energies (H_{298}, kcal/mol) of arynes at the CCSD(T) level of theory[a]

	Singlets						Triplets					
Molecules	2,3 *ortho*	2,4 *meta*	2,5 *para*	2,6 *meta*	3,4 *ortho*	3,5 *meta*	2,3 *ortho*	2,4 *meta*	2,5 *para*	2,6 *meta*	3,4 *ortho*	3,5 *meta*
Benzyne	31.2	17.5	5.7	(17.5)	(31.2)	(17.5)	−1.3	−0.6	3.0	(−0.6)	(−1.3)	(−0.6)
Pyridynium cations	22.5	19.4	4.3[b]	10.5	28.8	17.9	−2.7	−2.1	−1.3[b,c]	−1.6	−4.1	−1.7
Pyridynes	22.7	22.7	14.7	1.6[d]	32.7	16.2	3.8	−2.4	1.7	1.6	−1.8	1.7

[a] Results are for BPW91 geometries unless otherwise noted; thermal contributions to enthalpies from BPW91 level. For convenience, the relationship between the three benzyne isomers and the six pyridyne(ium) isomers is indicated and the benzyne results are multiply tabulated as necessary.

[b] BCCD(T) BSE.

[c] The CCSD(T) value is 0.7.

[d] CAS(8,8) geometry.

3.2. Comparison of the benzynes, pyridynes, and pyridynium cations

Analysis of trends in the data in Table 1 is difficult to the extent that the different zeros of energy [i.e. *o*-benzyne and the 3,4-pyridyne(ium) isomers] are not necessarily themselves directly comparable in terms of similar electronic structures, in spite of being isoelectronic. Further insights can be gained from alternative energetic analyses.

Table 2 details the ST splittings predicted for the various aryne isomers at the three different levels of theory surveyed here. Prior work on a variety of arynes suggests that the CCSD(T) level of theory is likely to be the most accurate of the three levels [16,21,53,62,63]. In the benzyne and pyridyne series, it has been shown that expanding the basis set to triple-ζ increases the magnitude of CCSD(T)-predicted ST splittings in *ortho* arynes by about 2.5 kcal/mol, whereas *meta* and *para* splittings are typically changed (either up or down) by less than 1 kcal/mol [21]; although we have not undertaken such calculations for the pyridynium cations, it seems likely that such corrections would similarly apply in generating the most accurate predictions for this series.

Table 3 provides, for the CCSD(T) level of theory using, for the most part, DFT geometries, the computed biradical stabilization energies (BSEs) for the different arynes, where BSE is defined as the predicted 298 K enthalpy of reaction for the isodesmic process

$$\text{arene} + m,n\text{-aryne} \rightarrow m\text{-aryl radical} + n\text{-aryl radical} \qquad (3)$$

i.e. it is the energy gained (or lost) from putting the two radical centers into the *same* aromatic ring. Earlier work has suggested that alternative isodesmic reactions may be more accurate for predicting 298 K heats of formation for *ortho* arynes [15,16,18], but for the sake of consistency, we will use only Eq. (3) here.

3.3. Ortho *isomers*

The 3,4-singlets and *o*-benzyne singlet all have very similar BSEs. Of the three, the BSE for 3,4-pyridynium is the smallest. We speculate that this is because the formal triple bond “locks” a certain degree of bond alternation into the six-membered ring, thereby decreasing the efficiency of resonance-derived charge delocalization.

The inference that introduction of a charged center into an aryne destabilizes isomers having dehydro positions adjacent to one another is further supported by the data for the 2,3-arynes, although the analysis is complicated somewhat by interactions of the lone pair in the singlet and triplet pyridynes. As has been previously noted [21], relative to the 2- and 3-pyridine monoradicals, a destabilizing four-electron interaction

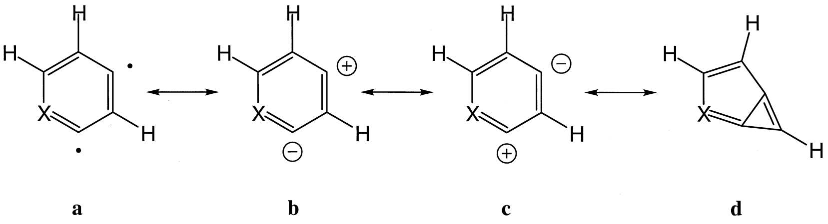

Fig. 4. Some resonance structures for 2,4-didehydroarynes.

between the in-plane π bond and the nitrogen lone pair decreases the BSE for the singlet 2,3-pyridyne, whereas the formation of an in-plane allyl-like delocalized set of orbitals stabilizes the triplet (so that it has a positive BSE of 3.8 kcal/mol). These interactions are not possible for the 2,3-pyridynium cations, which suggests that it is coincidence that the BSEs for 2,3-pyridyne and 2,3-pyridynium are similar—further consistent with the lack of strong interactions with the nitrogen lone pair is the “normal” negative BSE for the triplet. Note that this BSE is the next most negative after the already discussed 3,4-triplet, and is larger in magnitude than the BSE for triplet *o*-benzyne, again suggesting that charged systems disfavor adjacent dehydro positions relative to neutrals.

One item of interest is that the BSE for singlet 2,3-pyridynium is 6.3 kcal/mol smaller than the BSE for 3,4-pyridynium. This is somewhat counterintuitive since, if one indulges in drawing resonance structures, there would appear to be better opportunities for charge delocalization in the π system for the 2,3-isomer than for the 3,4-isomer. A careful analysis of geometric changes in the diradicals relative to the monoradicals suggests no special structural factors contributing to the predicted difference in stability. Mulliken population analysis of the DFT wave functions, however, suggests that the π resonance analysis represents an oversimplification of the charge-delocalization situation. The partial atomic charges on the NH fragments of the 2,3- and 3,4-isomers are 0.200 and 0.161, respectively, i.e. 20% less charge localization at nitrogen in the latter isomer. It would appear that inductive effects in the cationic system play a role in charge stabilization of similar magnitude to π delocalization effects. Thus, changing the formal hybridization at the two-position from sp^2 to the more electronegative *sp* destabilizes the 2,3-isomer relative to the 3,4-isomer.

The differences in singlet and triplet BSEs between the two *ortho* pyridynes and between the two *ortho* pyridyniums combine in each case to cooperatively decrease the magnitude of the 2,3 ST splitting relative to the 3,4 case. At the CCSD(T) level the difference between the two splittings is predicted to be 15.5 and 7.7 kcal/mol. Although this effect of heteroatomic substitution is sizable, it is noteworthy that it operates over a remarkably short range, insofar as both 3,4 splittings (where the nitrogen atom is one CH unit further from the formal triple bond) are predicted to essentially be the same as that computed for *o*-benzyne.

3.4. Meta *isomers*

Comparison of the *meta* diradicals is, at first glance, complicated by the preference for monocyclic structures in some systems and bicyclic structures in others. On the other hand, the remarkably flat nature of the potential coordinate associated with bond making/breaking between the two dehydro positions makes an energetic analysis in some sense independent of the structure, so comparison of BSEs remains a useful exercise.

Starting with the 2,4-isomers, Fig. 4 presents some aryne resonance structures that facilitate a discussion of differences between the three arynes. In the case of the triplets, only mesomer **a** is relevant (all other mesomers having formally closed-shell electronic structures), and the slightly smaller negative BSE for triplet *m*-benzyne compared to its pyridyne and pyri-

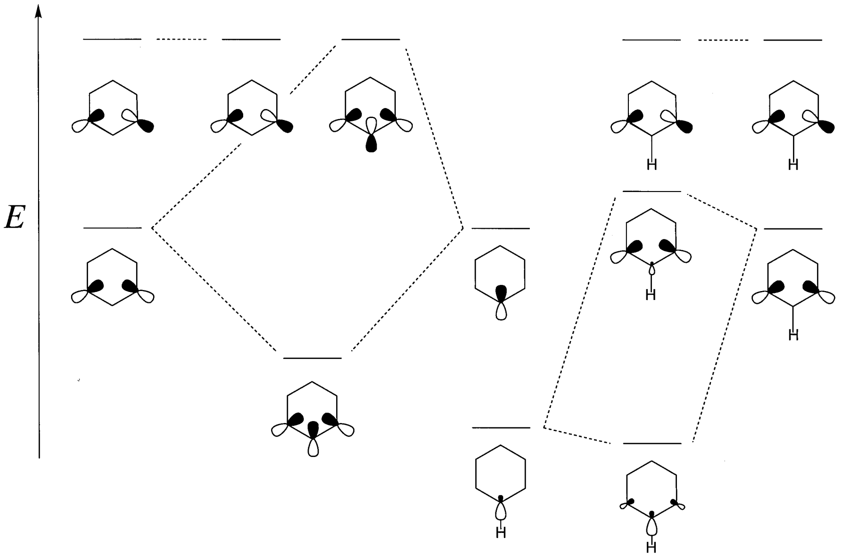

Fig. 5. Perturbative resonance analysis of in-plane allyl-like interactions for 2,6-pyridyne (left-hand half) and 2,6-pyridynium cation (right-hand half).

dynium analogs is probably attributable to the smaller ring size in the case of the heterocycles, which increases through-space interaction between the two centers and thereby slightly increases exchange repulsion (the separation between the two relevant carbon atoms is about 0.02 Å larger in benzene than in the other two arenes). Hoffmann et al. [12] predicted the direct interaction between these two centers for a model of *m*-benzyne to have a magnitude of 0.035β (where β is the standard resonance integral between two carbon sp^2 hybrid orbitals overlapping in a σ sense), although variation with respect to separation distance was not evaluated.

In the pyridynium *singlet* case, this same smaller separation described previously leads to ring closure, suggesting a dominance of mesomer **d** and a slightly larger positive BSE for 2,4-pyridynium compared to singlet *m*-benzyne. For 2,4-pyridyne, on the other hand, mesomer **c**, which has nitrilium ion character, can be a favorable contributor—as a result, this 2,4-aryne is predicted to have the most positive BSE of the 7 *meta* diradicals in this paper. We note that a more detailed analysis supporting the relevance of mesomer **c** in the latter aryne has been presented elsewhere [21].

The 2,6-arynes are particularly affected by the nature of the heteroatom (if any) because substitution dictating the ring's "one" position is necessarily adjacent to *both* of the dehydrocenters. Beginning again with a comparison of the triplets, once more the pyridynium BSE is somewhat more negative than the benzyne BSE, and again it is reasonable to ascribe this to the smaller heterocyclic ring (the 2,6-separation in pyridinium cation is 0.045 Å less than the equivalent separation in benzene). Triplet 2,6-pyridyne, on the other hand, has a small *positive* BSE. This has previously been assigned to the stabilization provided the latter diradical from the presence of an in-plane aza-allylic system formed from the nitrogen lone pair and the two dehydro sp^2 orbitals [21].

The 2,6-singlets show the largest variation in BSE across the three arynes, owing to the very small positive BSE predicted for the pyridyne case. As depicted in Fig. 5 (left-hand side), the relative destabilization of the singlet derives from an unfavorable four-electron interaction between the bonding combination of the dehydro-orbitals and the nitrogen lone pair [21]. This destabilization is so large that the antibonding hybrid orbital is comparable in energy to the antibonding singly-occupied molecular orbital of the triplet, and thus the ST gap in 2,6-pyridyne is predicted to be a mere 1.0 kcal/mol at the CCSD(T) level. When the lone pair is "bound up" with a proton, thereby making the orbital in question a N–H bond, it is sufficiently lowered in energy that resonance between it and the bonding didehydro hybrid is substantially reduced, although the BSE of singlet 2,6-pyridynium is still 7 kcal/mol smaller than that of singlet *m*-benzyne (right-hand side Fig. 5). In addition to possible resonance interactions, however, the cationic charge on the central NH fragment must contribute to some of the destabilization relative to *m*-benzyne, since any transfer of *s* character to the didehydro bonding orbital to lower its energy will be balanced by some unfavorable transfer of *s* character to the closely aligned C–N σ bond.

As for the 3,5-arynes, the triplets have essentially identical BSEs as predicted for the 2,6-arynes. The singlets, on the other hand, all have BSE values within 2 kcal/mol of each other. That the pyridyne congener has the smallest positive BSE may reflect some remaining destabilization from interaction with the lone pair (i.e. a similar analysis to that appearing on the left-hand side of Fig. 5, but the dehydro orbitals are moved to the three and five positions thereby decreasing resonance through reduced overlap), but the difference is small in any case.

3.5. Para *isomers*

Detailed comparisons of *p*-benzyne, 2,5-pyridyne, and 2,5-pyridynium have previously appeared [11,53], and this present study does not add anything substantive to these prior analyses. Interest in these particular diradicals derives from their potential use as reactive agents for the cleavage of DNA [2] when formed from Bergman cyclization of appropriate (aza) enediyne precursors [64]. For the sake of completeness, we summarize here the key points deriving from prior studies on these molecules.

First, the *p*-benzyne and 2,5-pyridynium singlets are very similar in all respects. Although the data in Tables 2 and 3 do not necessarily make this obvious, this derives in part from the failure of the CCSD(T) level when applied to 2,5-pyridynium; recourse to the BCCD(T) level is required because of instability engendered by large singles amplitudes in the standard CCSD expansion [53]. If the BCCD(T) level is applied to *p*-benzyne, the predicted ST splitting of −4.5 kcal/mol is in close agreement with the splitting of −5.6 kcal/mol predicted for 2,5-pyridynium.

Neutral 2,5-pyridyne, on the other hand, has a much larger ST splitting, owing primarily to a larger BSE associated with the singlet state. This additional stabilization for the pyridyne is attributable to energetically favorable mixing of a zwitterionic mesomer into the overall electronic structure as described above for 2,4-pyridyne [53]. As pointed out by Hoffner et al. [11], this difference in the ST splitting between protonated and unprotonated 2,5-pyridyne offers interesting opportunities for designing less cytotoxic antitumor agents, and experiment does suggest that whereas the protonated diradical is an avid hydrogen atom abstracting agent the neutral diradical, being a more stable singlet, is not [11,50].

3.6. An unusual Bergman cyclization

As just discussed, *para* arynes are readily generated from Bergman cyclization of appropriate enediynes. Most of the other diradicals discussed in this article, not being *para*, would require alternative methodologies—there is, however, one interesting exception. The 2,4-pyridyne diradical is in principle derivable as the product from a Bergman cyclization of *Z*-but-1-en-3-yn-1-yl isonitrile (Fig. 6). We have characterized the reaction coordinate for this process at the BPW91/cc-pVDZ level, and Fig. 6 provides some geometric details for the reactant and transition-state structure. Fig. 7 provides the 298 K activation enthalpy and overall enthalpy change for the reaction (reaction **iii**) along with data at the same level for five other previously studies Bergman cyclizations [53].

Previous studies on the Bergman cyclization of various enediynes have shown DFT to be reasonably robust for predicting cyclization barriers [53,59,61,79], owing to the very low degree of diradical character in the transition state [53,55,56,59,61]. It must be noted, however, that DFT can be less than ideal for predicting the overall reaction thermicity if the product diradical has a

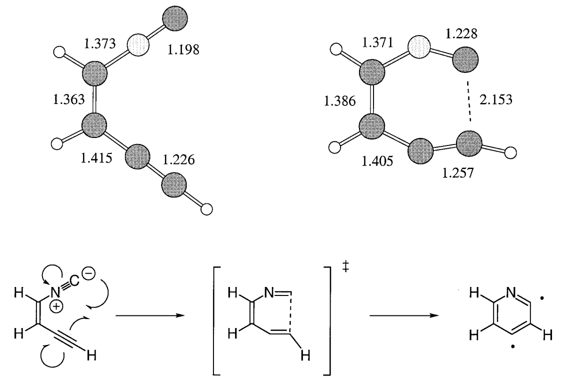

Fig. 6. Bergman cyclization of *Z*-but-1-en-3-yn-1-yl isonitrile. Heavy-atom bond lengths (angstroms) for the reactant and transition state structures at the BPW91/cc-pVDZ level are provided.

large degree of multiconfigurational character. As our intent is simply to provide some qualitative comparisons between this reaction and other characterized Bergman cyclizations, we restrict ourselves here to the efficient DFT level. We note that for the five other Bergman reactions listed in Fig. 7, by comparison to well converged levels of electronic structure theory (and also experiment in the case of reaction **i**), the DFT level underestimates the 298 K activation enthalpy by about 5 kcal/mol and predicts the overall cyclizations to be 5–10 kcal/mol more favorable than is correct [53]. Thus estimates of the activation enthalpy and exothermicity for the Bergman cyclization of *Z*-but-1-en-3-yn-1-yl isonitrile that may be assumed to be reasonably accurate are about 18 and 0 kcal/mol, respectively.

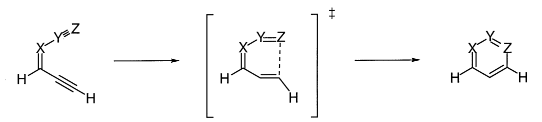

Reaction	X	Y	Z	$\Delta H^{\ddagger}_{298}$	ΔH^{rxn}_{298}
i	CH	C	CH	22.0	(0.9)
ii	CH	C	N	29.3	23.6
iii	CH	N	C	12.8	−7.3
iv	N	C	CH	14.5	−14.5
v	CH	C	NH^+	32.5	(22.4)
vi	NH^+	C	CH	18.3	(−6.9)

Fig. 7. Energetic comparison of different Bergman cyclizations. Predicted enthalpies of activation and reaction (298 K) are from the BPW91/cc-pVDZ level of theory. Reaction enthalpies in parentheses are from broken-spin-symmetry DFT calculations.

The transition state structure in Fig. 6 is similar to previously published structures at the same level for reactions **i**, **iv**, and **vi**; e.g. the forming C–C bond lengths in the latter three TS structures are 2.116, 2.272, and 2.163 Å, respectively [53]. (Reactions **ii** and **v** are unique in that the forming bond is a C–N bond, so direct comparison is not warranted.) From a structural standpoint, then, reaction **iii** is a "typical" Bergman cyclization. An energetic analysis, on the other hand, indicates reactions **ii** and **iii** to be possibly unique relative to the others.

Reaction **iii** is predicted to be the second most exothermic of the six reactions in Fig. 7; exothermicity is not necessarily unexpected given the comparatively low stability of an isonitrile compared to an alkyne or nitrile in the reactant. More interesting is that reaction **iii** has the lowest activation enthalpy of the six cyclizations. A more careful analysis indicates there to be an excellent linear relationship [80] between activation enthalpy and reaction thermicity for all of the reactions except for **ii** and **iii**, data points for both of which fall substantially below the line (Fig. 8). The inference then is that the activation enthalpies for these two reactions are lower than would be expected given their overall thermicities. These lower barriers are probably associated with the lack of a hydrogen atom on the isonitrile carbon or nitrile nitrogen compared to all of the other bond-forming termini in the remaining Bergman cyclizations. In the absence of unfavorable steric and/or other interactions involving the H atoms on the bond-forming termini, atomic orbital hybridizations need not change prior to the onset of favorable heavy-atom bonding interactions. Based on comparison to the correlating line in Fig. 8, this effect is worth 3–5 kcal/mol in reducing the activation enthalpy.

3.7. Hyperfine couplings as predictors for diradical ST splittings

Cramer and Squires [17] have reported that CASPT2/cc-pVDZ ST splittings in aryne diradicals correlate remarkably well with BPW91/cc-pVDZ monoradical ^1H hfs constants, where the hfs is computed for the hydrogen atom on the diradical position that is "capped" in the monoradical (one may assume

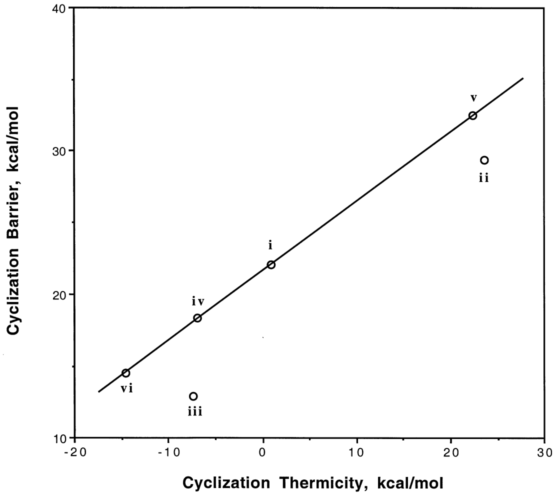

Fig. 8. Activation enthalpies vs. reaction thermicities (298 K) for the reactions listed in Fig. 7.

that the correlation with experiment might be of similarly high quality, but there are insufficient experimental data to correlate). For strongly interacting *ortho*- and *meta*-related diradicals (defined as having singlet ground states with ST gaps larger in magnitude than -10 kcal/mol), the regression equation, which has an R value of 0.997 when computed over 11 data points for relevant benzynes [17], pyridynes [21], and naphthalynes [17,19], is

$$(\text{ST splitting, kcal/mol}) = -1.39 \times ({}^{1}\text{H hfs, G}) - 9.48 \quad (4)$$

In the case of nonstrongly interacting *meta*- or *para*-related diradical centers, the correlating equation ($R = 0.987$, 9 data points) analogous to Eq. (4) is

$$(\text{ST splitting, kcal/mol}) = -1.99 \times ({}^{1}\text{H hfs, G}) - 0.30 \quad (5)$$

Note that Eq. (5) has a near-zero intercept, which meets with qualitative expectations that if a proton does not feel any unpaired electron spin density, an electron localized in the same position would not be expected to show much preference for singlet versus triplet coupling. The reason Eq. (5) differs so much from Eq. (4) is because weakly coupled diradicals in their singlet and triplet states and the monoradicals from which they might be generated typically all have very similar geometries. Thus, unpaired spin density in the monoradical may be regarded as a good measure of spin density from an electron at the same position in the diradical, and thus a zero intercept for the correlating line is expected. In the strongly coupled diradicals, on the other hand, there are typically large geometry differences between the individual states of the diradicals and/or between the diradicals and their related monoradicals. It is to some extent surprising that the correlation is as good as it is for Eq. (4), but that is the situation that obtains.

In any case, Table 4 lists the ST splittings predicted for the various pyridynium diradicals based on hfs values in the three pyridinium monoradicals. Comparison to CASPT2/cc-pVDZ predicted ST splittings (electronic energy only) indicates that the regression equations can be applied to the pyridynium series with an average error of about 1.6 kcal/mol. It is noteworthy that the largest errors are associated with the 2,4- and 3,5-isomers—both involve large geometric differences between bicyclic singlets and monocyclic triplets. Also worth noting is that hfs values from the 2-pyridinium radical are less predictive than those from the 3- or 4-pyridinium radicals for the same diradical (e.g. 2,4-pyridynium can be predicted from the hfs of proton 4 in the 2-radical or from the hfs of proton 2 in the 4-radical). This was observed previously for the congeneric unprotonated pyridine/pyridyne series [21] and seems to indicate a general trend for greater robustness in the correlations when the radical position in the monoradical is well insulated from strongly perturbing influences like lone pairs or formal charges.

3.8. Pyridyne 298 K heats of formation

In previous work [21], we reported the energies of the pyridyne singlets at an extrapolated level of coupled cluster theory defined as

$$\text{extrap. CCSD(T)} = \text{CCSD/cc-pVTZ} + [\text{CCSD(T)/cc-pVDZ} - \text{CCSD/cc-pVDZ}] \quad (6)$$

Table 4
Predicted and computed ST splittings (kcal/mol) for pyridynium diradicals[a]

	ST splitting					
Method	2,3	2,4	2,5	2,6	3,4	3,5
From 2-pyridinium radical hfs	−25.6	−19.5	−5.7[b]	−8.4[b]		
From 3-pyridinium radical hfs	−25.8		−4.5[b]		−32.5	−17.8
From 4-pyridinium radical hfs		−16.7			−32.4	
CASPT2/cc-pVDZ[c]	−23.9	−15.5	−5.1	−9.6	−31.5	−14.5

[a] Predictions are from Eq. (4) unless otherwise noted.
[b] From Eq. (5).
[c] Electronic energies only.

where all geometries were from the BPW91/cc-pVDZ level. In Eq. (6), then, the effect of triple excitations is evaluated with a smaller basis set than that used for the best CCSD calculation.

This level of theory has previously been shown to provide very accurate predictions for the 298 K heats of formation of the benzynes when used in conjunction with isodesmic Eq. (3) and the known heats of formation of benzene and the phenyl radical [16]. Heats of formation of the pyridyl radicals have recently been determined from analysis of shock tube experiments on pyridine [81]. By using those data and the heat of formation for pyridine, we have carried out analogous calculations of the 298 K heats of formation for all six pyridynes, and those are summarized in Table 5 along with a recapitulation of the benzyne results. As no C–H bond dissociation energies for protonated pyridine are available (nor are other estimates of protonated pyridyl radical heats for formation), we have not attempted to predict values for the pyridynium cations. The error estimate in the predicted column derives simply from the root mean square of the experimental uncertainties in the measured heats of formation and does not reflect any attempt to guess the intrinsic accuracy of the electronic structure calculations.

4. Conclusions

Introducing a nitrogen atom into the aromatic ring perturbs the structures and energies of the benzynes. This perturbation is much larger for the singlet states than for the triplet states, and is also larger when the nitrogen atom is unprotonated than when it is protonated and the aryne is a cation. The nitrogen lone pair in the pyridynes strongly hybridizes with one or both of the nonbonding sigma orbitals if the latter is (are)

Table 5
Computed H_{298} (a.u.) and experimental and computed $\Delta H^{\text{o}}_{\text{f},298}$ (kcal/mol) values

		$\Delta H^{\text{o}}_{\text{f},298}$	
Molecule	H_{298}[a]	Experimental	Predicted[b]
Benzene	−231.685 12	19.7 ± 0.2[c]	
Phenyl radical	−231.006 56	81.2 ± 0.6[d]	
Pyridine	−247.722 33	33.6 ± 0.2[c]	
2-Pyridyl radical	−247.051 44	86 ± 2	
3-Pyridyl radical	−247.042 22	93 ± 2	
4-Pyridyl radical	−247.044 61	93 ± 2	
o-Benzyne	−230.381 55	105.9 ± 3.3[e]	109.0 ± 0.9
m-Benzyne	−230.359 71	121.9 ± 3.1[f]	122.7 ± 0.9
p-Benzyne	−230.336 59	137.8 ± 2.9[f] 138.0 ± 1.0[g]	137.2 ± 0.9
2,3-Pyridyne	−246.411 26		121 ± 3
2,4-Pyridyne	−246.411 23		123 ± 3
2,5-Pyridyne	−246.395 06		131 ± 3
2,6-Pyridyne[h]	−246.383 88		137 ± 3
3,4-Pyridyne	−246.419 87		118 ± 3
3,5-Pyridyne	−246.391 98		135 ± 3

[a] Electronic energies at extrap. CCSD//BPW91/cc-pVDZ level unless otherwise specified; see Eq. (6). ZPVE and thermal contributions from BPW91/cc-pVDZ level.
[b] For singlet diradicals by using Eq. (3) and experimental $\Delta H^{\text{o}}_{\text{f},298}$ values for arenes and arenyl radicals.
[c] See [82].
[d] See [44].
[e] See [51].
[f] See [44,83].
[g] See [43].
[h] Electronic energy at extrap. CCSD//CAS/cc-pVDZ level.

localized on one or both of the carbon atoms adjacent to the nitrogen atom. Such hybridization can stabilize the singlet state by making zwitterionic resonance structures more favorable than would be the case for benzyne isomers. Introduction of a positive charge, in the form of a protonated nitrogen, can also influence singlet energies, primarily by inductive effects propagated through the σ framework of the aromatic ring. There is also a bias towards maintaining structures that maximize π delocalization in the charged arynes.

The Bergman cyclization of *Z*-but-1-en-3-yn-1-yl isonitrile is unique insofar as it produces a *meta* diradical, namely 2,4-pyridyne. The cyclization itself is exothermic, and overall similar to other computationally characterized Bergman processes for acyclic azaenediynes, except that it exhibits a somewhat smaller barrier that is associated with the lack of a terminal hydrogen at the isonitrile carbon atom.

Proton hyperfine splittings in protonated pyridine monoradicals are good predictors of singlet-triplet splittings in didehydropyridynium diradicals, in keeping with prior observations in other aryne systems. When singlet states adopt bicyclic geometries, however, the predictive utility of the hyperfine splittings is reduced.

Acknowledgements

The authors are grateful for high-performance computing resources, as well as an undergraduate internship, made available by the Minnesota Supercomputer Institute. This work was supported in part by the National Science Foundation, the Alfred P. Sloan Foundation, and the University of Minnesota's Undergraduate Research Opportunities Program (UROP).

References

[1] Enediyne Antibiotics as Antitumor Agents, D.B. Borders, T.W. Doyle (Eds.) Marcel Dekker, New York, 1995.
[2] K.C. Nicolaou, W.-M. Dai, Angew. Chem. 103 (1991) 1453.
[3] R. Poon, T.A. Beerman, I.H. Goldberg, Biochemistry 16 (1977) 486.
[4] A.G. Myers, S.B. Cohen, B.-M. Kwon, J. Am. Chem. Soc. 116 (1994) 1670.
[5] A.G. Myers, E.Y. Kuo, N.S. Finney, J. Am. Chem. Soc. 111 (1989) 8057.
[6] A.G. Myers, C.A. Parrish, Bioconjugate Chem. 7 (1996) 322.
[7] I.H. Goldberg, L.S. Kappen, Y.-j. Xu, A. Stassinopoulos, X. Zeng, Z. Xi, C.F. Yang, in DNA and RNA Cleavers and Chemotherapy of Cancer and Viral Diseases, B. Meunier (Ed.), Kluwer, Amsterdam, 1996, p. 1.
[8] P. Chen, Angew. Chem. 108 (1996) 1584.
[9] C.F. Logan, P. Chen, J. Am. Chem. Soc. 118 (1996) 2113.
[10] M.J. Schottelius, P. Chen, J. Am. Chem. Soc. 118 (1996) 4896.
[11] J. Hoffner, M.J. Schottelius, D. Feichtinger, P. Chen, J. Am. Chem. Soc. 120 (1998) 376.
[12] R. Hoffmann, A. Imamura, W.J. Hehre, J. Am. Chem. Soc. 90 (1968) 1499.
[13] S.G. Wierschke, J.J. Nash, R.R. Squires, J. Am. Chem. Soc. 115 (1993) 11958.
[14] A. Nicolaides, W.T. Borden, J. Am. Chem. Soc. 115 (1993) 11951.
[15] R. Lindh, M. Schütz, Chem. Phys. Lett. 258 (1996) 409.
[16] C.J. Cramer, J.J. Nash, R.R. Squires, Chem. Phys. Lett. 277 (1997) 311.
[17] C.J. Cramer, R.R. Squires, J. Phys. Chem. A 101 (1997) 9191.
[18] R. Lindh, A. Bernhardsson, M. Schütz, J. Phys. Chem. A 103 (1999) 9913.
[19] R.R. Squires, C.J. Cramer, J. Phys. Chem. A 102 (1998) 9072.
[20] H.H. Nam, G.E. Leroi, J.F. Harrison, J. Phys. Chem. 95 (1991) 6514.
[21] C.J. Cramer, S. Debbert, Chem. Phys. Lett. 287 (1998) 320.
[22] J.G. Bunnett, T.K. Brotherton, J. Am. Chem. Soc. 78 (1956) 155.
[23] J.D. Roberts, D.A. Semenow, H.E. Simmons, L.A. Carlsmith, J. Am. Chem. Soc. 78 (1956) 601.
[24] T.L. Gilchrist, C.W. Rees, Carbenes, Nitrenes, and Arynes, Nelson, London, 1969.
[25] T. Kauffmann, R. Wirthwein, Angew. Chem., Int. Ed. Engl. 10 (1971) 20.
[26] N. Darby, C.U. Kim, J.A. Salaün, K.W. Shelton, S. Takada, S. Masamune, J. Chem. Soc. Chem. Commun. (1972) 1516.
[27] R.R. Jones, R.G. Bergman, J. Am. Chem. Soc. 94 (1972) 660.
[28] M.R. Bryce, J.M. Vernon, Adv. Heterocycl. Chem. 28 (1981) 183.
[29] C. Wentrup, Reactive Molecules, Wiley, New York, 1984, p. 288.
[30] R.H. Levin, in Reactive Intermediates, Vol. 3, M. Jones, R. Moss (Eds.), Wiley, New York, 1985, p. 1.
[31] H.H. Nam, G.E. Leroi, J. Am. Chem. Soc. 110 (1988) 4096.
[32] M.A. Bennett, H.P. Schwemlein, Angew. Chem., Int. Ed. Engl. 28 (1989) 1296.
[33] G. Just, R. Singh, Tetrahedron Lett. 31 (1990) 185.
[34] K.N. Bharucha, R.M. Marsh, R.E. Minto, R.G. Bergman, J. Am. Chem. Soc. 114 (1992) 3120.
[35] A.G. Myers, N.S. Finney, J. Am. Chem. Soc. 114 (1992) 10986.
[36] K.N. Bharucha, R.M. Marsh, R.E. Minto, R.G. Bergman, J. Am. Chem. Soc. 114 (1992) 3120.

[37] A.G. Myers, P.S. Dragovich, J. Am. Chem. Soc. 115 (1993) 7021.
[38] D.L. Boger, J. Zhou, J. Org. Chem. 58 (1993) 3018.
[39] J. Averdung, J. Mattay, Tetrahedron Lett. 35 (1994) 6661.
[40] H.V. Linnert, J.M. Riveros, Int. J. Mass Spectrom. Ion. Processes 140 (1994) 163.
[41] M.F. Semmelhack, T. Neu, F. Foubelo, J. Org. Chem. 59 (1994) 5038.
[42] P. Wenthold, R.R. Squires, J. Am. Chem. Soc. 116 (1994) 6401.
[43] W.R. Roth, H. Hopf, C. Horn, Chem. Ber. 127 (1994) 1765.
[44] G.E. Davico, V.M. Bierbaum, C.H. DePuy, G.B. Ellison, R.R. Squires, J. Am. Chem. Soc. 117 (1995) 2590.
[45] H.A. Weimer, B.J. McFarland, S. Li, W. Weltner, J. Phys. Chem. 99 (1995) 1824.
[46] W.R. Roth, H. Hopf, T. Wasser, H. Zimmerman, C. Werner, Liebigs Ann. Chem. (1996) 1691.
[47] J.J. Nash, R.R. Squires, J. Am. Chem. Soc. 118 (1996) 11872.
[48] K.K. Wang, Chem. Rev. 96 (1996) 207.
[49] K.K. Thoen, H.I. Kenttämaa, J. Am. Chem. Soc. 119 (1997) 3832.
[50] W.M. David, S.M. Kerwin, J. Am. Chem. Soc. 119 (1997) 1464.
[51] P.G. Wenthold, R.R. Squires, W.C. Lineberger, J. Am. Chem. Soc. 120 (1998) 5279.
[52] K.K. Thoen, H.I. Kenttämaa, J. Am. Chem. Soc. 121 (1999) 800.
[53] C.J. Cramer, J. Am. Chem. Soc. 120 (1998) 6261.
[54] A.C. Scheiner, H.F. Schaefer III, B. Liu, J. Am. Chem. Soc. 111 (1989) 3118.
[55] E. Kraka, D. Cremer, J. Am. Chem. Soc. 116 (1994) 4929.
[56] R. Lindh, T.J. Lee, A. Bernhardsson, B.J. Persson, G. Karlström, J. Am. Chem. Soc. 117 (1995) 7186.
[57] E. Kraka, D. Cremer, G. Bucher, H. Wandel, W. Sander, Chem. Phys. Lett. 268 (1997) 313.
[58] J. Gräfenstein, E. Kraka, D. Cremer, Chem. Phys. Lett. 288 (1998) 593.
[59] P.R. Schreiner, Chem. Commun. (1998) 483.
[60] H.J. Jiao, P.V. Schleyer, B.R. Beno, K.N. Houk, R. Warmuth, Angew. Chem., Int. Ed. Engl. 36 (1998) 2761.
[61] P.R. Schreiner, J. Am. Chem. Soc. 120 (1998) 4184.
[62] C.J. Cramer, R.R. Squires, Org. Lett. 1 (1999) 215.
[63] C.J. Cramer, J. Chem. Soc. Perkin Trans. 2, (1999) 2273.
[64] R.G. Bergman, Accounts Chem. Res. 6 (1973) 25.
[65] T.H. Dunning, J. Chem. Phys. 90 (1989) 1007.
[66] M.W. Schmidt, M.S. Gordon, Annu. Rev. Phys. Chem. 49 (1998) 233.
[67] A.D. Becke, Phys. Rev. A 38 (1988) 3098.
[68] J.P. Perdew, K. Burke, Y. Wang, Phys. Rev. B 54 (1996) 16533.
[69] W. Sander, H. Wandel, G. Bucher, J. Grafenstein, E. Kraka, D. Cremer, J. Am. Chem. Soc. 120 (1998) 8480.
[70] K. Andersson, P.-Å. Malmqvist, B.O. Roos, A.J. Sadlej, K. Wolinski, J. Phys. Chem. 94 (1990) 5483.
[71] K. Andersson, B.O. Roos, Int. J. Quantum Chem. 45 (1993) 591.
[72] K. Andersson, M.R.A. Blomberg, M.P. Fülscher, G. Karlström, V. Kellö, R. Lindh, P.-Å. Malmqvist, J. Noga, J. Olsen, B.O. Roos, A.J. Sadlej, P.E.M. Siegbahn, M. Urban, P.-O. Widmark, MOLCAS-3, University of Lund, Sweden, 1994.
[73] G.D. Purvis, R.J. Bartlett, J. Chem. Phys. 76 (1982) 1910.
[74] K. Raghavachari, G.W. Trucks, J.A. Pople, M. Head-Gordon, Chem. Phys. Lett. 157 (1989) 479.
[75] N. Handy, J.A. Pople, M. Head-Gordon, K. Raghavachari, G.W. Trucks, Chem. Phys. Lett. 164 (1989) 185.
[76] J.F. Stanton, Chem. Phys. Lett. 281 (1997) 130.
[77] M.H. Lim, S.E. Worthington, F.J. Dulles, C.J. Cramer, in Density-Functional Methods in Chemistry, ACS Symposium Series, Vol. 629, B.B. Laird, R.B. Ross, T. Ziegler (Eds.), American Chemical Society, Washington, DC, 1996, p. 402.
[78] M.J. Frisch, G.W. Trucks, H.B. Schlegel, P.M.W. Gill, B.G. Johnson, M.A. Robb, J.R. Cheeseman, T.A. Keith, G.A. Petersson, J.A. Montgomery, K. Raghavachari, M.A. Al-Laham, V.G. Zakrzewski, J.V. Ortiz, J.B. Foresman, C.Y. Peng, P.A. Ayala, M.W. Wong, J.L. Andres, E.S. Replogle, R. Gomperts, R.L. Martin, D.J. Fox, J.S. Binkley, D.J. Defrees, J. Baker, J.P. Stewart, M. Head-Gordon, C. Gonzalez, J.A. Pople, GAUSSIAN 94, RevE.2, Gaussian Inc., Pittsburgh, PA, 1995.
[79] R. Lindh, U. Ryde, M. Schütz, Theor. Chem. Acc. 97 (1997) 203.
[80] L.P. Hammett, Chem. Rev. 17 (1935) 125.
[81] J.H. Kiefer, Q. Zhang, R.D. Kern, J. Yao, B. Jursic, J. Phys. Chem. A 101 (1997) 7061.
[82] J.B. Pedley, R.D. Naylor, S.P. Kirby, Thermochemical Data of Organic Compounds, Chapman and Hall, New York, 1986.
[83] P.G. Wenthold, J. Hu, R.R. Squires, J. Am. Chem. Soc. 116 (1994) 6961.